Exploring the electronic and optical properties of Cu2Sn1-xGexS3 and Cu2Sn1-xSixS3 (x = 0, 0.5, and 1)

Rongzhen Chen[*, 1, 2] and Clas Persson[1, 2, 3]

1 Department of Materials Science and Engineering, KTH Royal Institute of Technology, SE-100 44 Stockholm, Sweden
2 Centre for Materials Science and Nanotechnology, University of Oslo, P.O. Box 1048 Blindern, NO-0316 Oslo, Norway
3 Department of Physics, University of Oslo, P.O. Box 1048 Blindern, NO-0316 Oslo, Norway

In order to accelerate for environmental friendly thin-film photovoltaic industry, earth-abundant, non-toxic, and low-cost absorber materials are demanded. We study the compounds of $Cu_2Sn_{1-x}Ge_xS_3$ and $Cu_2Sn_{1-x}Si_xS_3$ (x = 0, 0.5, and 1) employing first-principles method within the density functional theory. Comparable band dispersions for all compounds are found. Moreover, the band-gap energies E_g of those materials can be tailored by cation alloying the Sn atoms with Ge or Si. The gap energies of $Cu_2Sn_{1-x}Ge_xS_3$ and $Cu_2Sn_{1-x}Si_xS_3$, with x = 0, 0.5, and 1, vary almost linearly from 0.83 to 1.43 and 2.60 eV, respectively. However, the gap energy of Cu_2SiS_3 does not follow the linear relation for $x > 0.8$. The effective electron masses of lowest conduction band at the Γ-point are relatively isotropic for all materials, which are between 0.15 and 0.25 m_0 in (010) direction, and between 0.13 and 0.22 m_0 in (001) direction. On the other hand, the effective hole masses of topmost valence band at the Γ-point show very strong anisotropy for all compounds. In the (010) direction, the hole masses are estimated to be between 1.01 and 1.85 m_0, while between 0.11 and 0.41 m_0 in the (001) direction. Calculations reveal that all compounds have relatively high absorption coefficients, comparable with that of Cu_2ZnSnS_4. However, the absorption coefficients in the energy region E_g + 0.5 to E_g + 1 eV are higher for Cu_2GeS_3, Cu_2SiS_3, and $Cu_2Sn_{0.5}Si_{0.5}S_3$ compared with Cu_2ZnSnS_4. Here, a dense **k**-mesh is required in order to observe the details of absorption spectra, especially near band-gap region. The high-frequency dielectric constants of all compounds are between 6.2 and 7.5, which are similar to the one of Cu_2ZnSnS_4 (~6.7). Therefore, $Cu_2Sn_{1-x}Ge_xS_3$ and $Cu_2Sn_{1-x}Si_xS_3$ can be potential candidates as absorber materials in thin-film solar cells.

1 Introduction

$Cu(In, Ga)Se_2$ (CIGS) is one of the most important thin-film photovoltaic (PV) material [1]. However, the cost of In and Ga, scarcity of In, as well as toxicity of Se are limiting the expansion of PV industry using CIGS. In recent years, $Cu_2ZnSn(S,Se)_4$ (CZTSSe) have attracted increasing attention due to the earth abundant elements in the compound, and the best efficiency already reached 12.6% [2]. In addition, CZTSSe has a relatively high absorption coefficient, which is an important feature as a thin-film absorber material. One disadvantage of CZTSSe is the toxicity of Se. Hence, the search of alternatively solar cell materials is still an ongoing active area today. To overcome all above-mentioned problems, the ternary chalcogenide semiconductor Cu_2MS_3 (where M = Sn, Ge, and Si) and their alloys are suggested [3-9]. Cu_2SnS_3 (CTS), with monoclinic structure, is considered as an absorber material, and the conversion efficiencies of 4.63% and 4.29% are obtained by Nakashima *et al*. [3] and by Kanai *et al*. [4], respectively. Theoretically, the band-gap energy of CTS is estimated to be between 0.8 and 0.9 eV [5], which is in good agreement with experimental data [6, 7]. Since Ge and Si are group-IV elements as Sn, it is expected to tailor the band-gap energies by alloying Sn in CTS by Ge or Si. By alloying Sn by Ge, Umehara *et al*. fabricated a solar cell using $Cu_2Sn_{0.83}Ge_{0.17}S_3$, and the cell efficiency of 6.0% was reported [8]. The band-gap energy is ~1.0 eV for this compound. Araki *et al*. synthesized a solar cell using Cu_2GeS_3 (CGS) as an absorber, which has an efficiency of 1.70%, and the gap of CGS is between 1.5 and 1.6 eV [9]. The band-gap energy of Cu_2SiS_3 (CSS) is as high as 2.56 eV, but alloying Sn with Si the band-gap energies of $Cu_2Sn_{0.5}Si_{0.5}S_3$ decreases to 1.40 eV according to measurements by Toyonaga *et al*. [6]. To our knowledge, there is no PV cell fabricated based on compounds alloying Sn with Si in CTS. Nevertheless, $Cu_2Sn_{1-x}Ge_xS_3$

(CTGS) and $Cu_2Sn_{1-x}Si_xS_3$ (CTSS) are environmentally benign materials. Also, the band-gap of all materials can be tailored in a wide range; hence the open-circuit voltage of corresponding PV cell can be optimized. However, today the experimental efficiencies are rather low considering that the compounds as absorber materials. Thus, it is important to understand the fundamental physical properties of these compounds.

In this work, the electronic and optical properties of CTGS and CTSS are theoretically explored by first-principles density functional theory (DFT) calculations. We report that all the compounds have direct band gap, and the gap energies can be tailored by alloying Sn by Ge or Si. The gap energies of CTGS and CTSS where x = 0, 0.5, 1 are almost linearly increased from 0.83 to 1.43 and 2.60 eV, respectively. However, the gap of CSS does not follow the linear trend of CTSS for large x, i.e. Si-rich alloy. Furthermore, the effective electron masses are isotropic, and hole masses are anisotropic. The spectra of absorption coefficients of all compounds are similar to the one of Cu_2ZnSnS_4 (CZTS). However, compared with absorption of CZTS, stronger absorptions are observed for CGS, CSS, and $Cu_2Sn_{0.5}Si_{0.5}S_3$ for low energy photon absorption. Furthermore, we suggest that it is essential to consider dense **k**-mesh for the calculations in order to show the details of absorption coefficients, especially in the vicinity of band-gap.

2 Computational details

The electronic and optical properties are theoretically calculated by means of the plane augmented wave formalism within the DFT as implemented in the VASP program package [10, 11]. We model the monoclinic Cu_2MS_3 (M = Sn, Ge, and Si) with a 12 atoms primitive cell. The compounds of $Cu_2Sn_{0.5}Ge_{0.5}S_3$ and $Cu_2Sn_{0.5}Si_{0.5}S_3$ are modeled by substituting one Sn by Ge or Si. Supercell with 48 atoms is utilized to confirm the convergence of the calculations using 12 atoms cell. The electronic structure and absorption spectra are analyzed by Heyd-Scuseria-Ernzerhof screened hybrid functional (HSE06) [12] with N_k = 39 **k**-points in the irreducible Brillouin zone (IBZ). The lattice constants and the atom positions are fully relaxed using the HSE06 potential until the total energy and the residual force on each atom converge to 0.1 meV and 10 meV/ Å, respectively.

In addition, optical properties with dense **k**-mesh (N_k = 6992 **k**-points) are calculated using the generalized gradient approximation (*i.e.*, PBE [13]) with a correction potential of *d*-like orbitals (PBE+U_d) [14], where U_d(Cu) = 6 eV and U_d(Zn) = 7.5 eV on the Cu and Zn atoms [15,16], respectively.

3 Results and discussion

3.1 Crystal structure

The ternary Cu_2MS_3 compounds where M = Sn, Ge, and Si crystallize in monoclinic structure (Cc; space group no. 9) [6, 9]. There are 12 atoms in the primitive cell. Each Cu or M atom is surrounded by 4 S atoms. The calculated lattice constants of Cu_2MS_3 and their alloys, using HSE06, are given in Table 1; this agree fairly well with available experimental data. For example, the relaxed (experimental) lattice parameters of CGS are a = 6.45 (6.44) Å, b = 11.29 (11.32) Å, c = 6.44 (6.43), and β = 108.71 (108.37) ° [17]. However, to our knowledge, experimental lattice information of $Cu_2Sn_{0.5}Ge_{0.5}S_3$ does not exist in the literature. The linear relation of lattice constants is found for CTGS and CTSS.

3.2 Electronic properties

The electronic band structure and atomic- and angular-momentum-dependent density-of-states (PDOS) are presented in Fig. 1. Overall, all compounds have rather similar band dispersion and PDOS, especially below the valence band maximum (VBM). Similar to CIGS and CZTSSe, the compounds of CTGS (x = 0, 0.5, and 1), Cu *d*-like states hybridize with S *p*-like states below VBM in a broad energy range. From the conduction band minimum (CBM) to about CBM + 1.7 eV, Sn or/and Ge *s*- like states mainly hybridize with S *p*-like states. For the $Cu_2Sn_{0.5}Ge_{0.5}S_3$ alloy, mixture of Sn and Ge *s*-like states hybridizes

with S *p*-like states. Therefore, the trends of the gap and the PDOS with respect to alloying concentrations are obvious for CTGS. For compounds of CTSS (x = 0, 0.5, and 1), Sn and Si *s*-like states of $Cu_2Sn_{0.5}Si_{0.5}S_3$ are not obviously mixed as Sn and Ge *s*-like states in $Cu_2Sn_{0.5}Ge_{0.5}S_3$, but a hybridization with S *p*-like states is found. Notice that the second lowest conduction band (CB) in $Cu_2Sn_{0.5}Si_{0.5}S_3$ is lifted up compared with the one of $Cu_2Sn_{0.5}Ge_{0.5}S_3$.

Calculated effective masses, in the (010) and (001) directions are presented in Table 2. Overall, for each compound, the effective electron masses of the lowest conduction band are almost isotropic at the Γ-point. Furthermore, the effective electron masses are small and apparently isotropic for all materials. The mass values are all between (0.15–0.25)m_0 in the (010) direction and between (0.13–0.22)m_0 in the (001) direction, and the masses are thus comparable to the electron mass of CZTS ($m_e \approx 0.18m_0$) [18]. However, the effective hole masses, in the two directions, of topmost valence band (VB) are strong anisotropic for each material. For instance, hole mass is $1.85m_0$ in (010) direction, but $0.11m_0$ in (001) direction. It may imply that the compounds has a better electron mobility than hole mobility. It is also noted that the effective electron masses are increased for CTGS and CTSS with x = 0, 0.5, and 1 except CSS and $Cu_2Sn_{0.5}Si_{0.5}S_3$ in (001) direction. The effective hole masses are increased for CTGS and CTSS with x = 0, 0.5, and 1 in (001) direction, but decreased in (010) direction.
In Fig. 2, the bands-gap energies E_g of CTGS and CTSS (x = 0, 0.25, 0.5, 0.75, and 1) are presented. Here, the compounds with x = 0.25 and 0.75 are modeled using supercells with 48 atoms. We report that the gap energies of CTGS vary almost linearly from 0.83 to 1.43 eV. The gaps of CTSS (x = 0, 0.25, 0.5, and 0.75) are almost linearly increased as well. However, the gap energy of pure CSS is surprisingly large and does not follow the linear trend. This is confirmed by experimental measurement [6]. The trend of the calculated gap energies is rather comparable to the one from experimental measurements by XX, et al. XX et al. and XX et al. [6, 8, 9].

3.3 Optical properties

The calculated absorption coefficients of CTGS and CTSS are shown in Fig. 3. The results in Fig. 3(a) are obtained from the HSE06 calculation with a sparse **k**-mesh of N_k = 39 **k**-points in the IBZ, which normally generates spectra that are qualitatively in good agreement with measurements over a large energy range. However, in order to reveal details of the optical properties, a much denser **k**-mesh is required [15]. Calculations from PBE+U_d with N_k = 6992 **k**-points in the IBZ are therefore considered [see Fig. 3(b)], and the gap energies are shifted by Δ_g, which is the difference between the gap energies of HSE06 and PBE+U_d. Hence, the same gap energies, as obtained from HSE06, can be seen in Fig. 3(b). In the two inset figures, the absorption coefficients are presented by shifting the energy scale to $\hbar\omega - E_g$.

In Fig. 3, HSE06 and PBE+U_d yield rather similar absorption coefficients for all compounds. However, from the inset figures, weaker and stronger responds, just above the band gap, can be observed from HSE06 with fine **k**-mesh and PBE+U_d with dense **k**-mesh, respectively. The stronger respond in CTS is consistent with the experimental finding [15]. Hence, we believe that dense **k**-mesh is essential to analyse the details of optical properties. The peaks of absorption coefficients can be identified by the transitions from some VB to CB. For instance, the peak around 3.2 eV of CSS in Fig. 3(a) may originate from the transition between topmost VB and second lowest CB near the Γ-point; the peak near 2.5 eV for $Cu_2Sn_{0.5}Si_{0.5}S_3$ may from the contribution from second topmost VB to lowest CB at the *A*-point (see Fig. 1). For comparison, the absorption coefficient of kesterite CZTS is presented in Fig. 3. Overall, the absorptions are rather similar between all the compounds and CZTS in a broad range of energy. However, in the inset figures, higher absorptions of CGS, CSS, and $Cu_2Sn_{0.5}Si_{0.5}S_3$ are observed around between E_g + 0.5 eV and E_g + 1.0 eV. Explain why that good!!!

The calculated high-frequency of dielectric constants, using HSE06, are 7.5, 7.2, and 7.1 for CTGS with x = 0, 0.5, and 1. CTSS has slightly larger dielectric constants: 6.7 and 6.2 for x = 0.5 and 1, respectively.

As expected, compounds with higher dielectric constants have lower gap energies. However, all the values are comparable to that of CZTS (~6.7) [18].

4 Conclusions

To conclude, the electronic and optical properties of CTGS and CTSS are investigated using first-principles calculations. The band-gap energies can be tailored and optimized by alloying Sn by Ge or Si. The gap energies are 0.83, 1.14, and 1.43 eV for CTGS with x = 0, 0.5, and 1, respectively. Corresponding energies for CTSS are 0.83, 0.15 and 2.60 eV. The linear relation of gap energies is observed for all materials except for CSS at large x. From the analysis of effective masses in two symmetry directions, we expect that effective electron masses of all materials are almost isotropic. However, effective hole masses are rather anisotropic. The materials may therefore have better electron mobility than hole mobility. The absorption coefficients of all compounds are comparable with the one of CZTS. Especially, higher absorptions can be observed around between E_g + 0.5 eV and E_g + 1.0 eV for CGS, CSS, and $Cu_2Sn_{0.5}Si_{0.5}S_3$. Hence, CTGS and CTSS can be considered as potential absorber materials.

Acknowledgements

This work is supported by the Re-search Council of Norwegian (projects 243642 and 221469). We acknowledge high-performance computer re-sources at NSC and USIT through SNIC/SNAC and NO-TUR.

References

[1] M. D. Archer and M. A. Green, Clean Electricity from Pho-tovoltaics 2nd Edition (Imperial, London, 2014), p. 245.

[2] W. Wang, M. T. Winkler, O. Gunawan, T. Gokmen, T. K. Todorov, Y. Zhu, and D. B. Mitzi, Adv. Energy Mater. 4, 1301465 (2014).

[3] M. Nakashima, J. Fujimoto, T. Yamaguchi, and M. Izaki, Appl. Phys. Express 8, 042303 (2015).

[4] A. Kanai, K. Toyonaga, K. Chino, H. Katagiri, and H. Arki, Jpn. J. Appl. Phys. 54, 08K06 (2015).

[5] Y. T. Zhai, S. Chen, J. H. Yang, H. J. Xiang, X. G. Gong, A. Walsh, J. Kang, S. H. Wei, Phys. Rev. B 84, 075213 (2011).

[6] K. Toyonaga and H. Araki, Phys. Status Solidi C 12, 753 (2015).

[7] D. M. Berg, R. Djemour, L. Gütay, G. Zoppi, S. Siebentritt, and P. J. Dale, Thin Solid Films 520, 6291 (2012).

[8] M. Umehara, Y. Takeda, T. Motohiro, T. Sakai, H. Awano, and R. Maekawa, Appl. Phys. Express 6, 045501 (2013).

[9] H. Araki, K. Chino, K. Kimura, N. Aihara, K. Jimbo, and H. Katagiri, Jpn. J. Appl. Phys. 53, 05FW10 (2014).

[10] G. Kresse and D. Joubert, Phys. Rev. B 59, 1758 (1999).

[11] G. Kresse and J. Furthmüller, Phys. Rev. B 54, 1169 (1996).

[12] J. Heyd, G. E. Scuseria, and M. Ernzerhof, J. Chem. Phys. 118, 8207 (2003).

[13] J. P. Perdew, K. Burke, and M. Ernzerhof, Phys. Rev. Lett. 77, 3865 (1996).

[14] V. I. Anisimov, J. Zaanen, and O. K. Andersen, Phys. Rev. B 44, 943 (1991).

[15] A. Crovetto, R. Chen, R. B. Ettlinger, A. C. Cazzaniga, J. Schou, C. Persson, and O. Hansen, Sol. Energy Mat. Sol. Cells 154, 121 (2016).

[16] W. Setyawan, R. M. Gaume, S. Lam, R. S. Feigelson, and S.Curtarolo, ACS Comb. Sci. 13, 382 (2011).

[17] L. M. de Chalbaud, G. D. de Delgado, J. M. Delgado, A. E. Mora, and V. Sagredo, Mater. Res. Bull. 32, 1371 (1997).

[18] C. Persson, J. Appl. Phys. 107, 053710 (2010).

Table 1 Calculated lattice information of $Cu_2Sn_{1-x}Ge_xS_3$ and $Cu_2Sn_{1-x}Ge_xS_3$. Experimental values are presented in the brackets.

Compound	*a* [Å]	*b* [Å]	*c* [Å]	*β* [°]
Cu_2SnS_3	6.67 (6.65[a])	11.57 (11.53[a])	6.68 (6.66[a])	109.41 (109.38[a])
Cu_2GeS_3	6.45 (6.44[b])	11.29 (11.32[b])	6.44 (6.43[b])	108.71 (108.37[b])
Cu_2SiS_3	6.34 (6.33[a])	11.21 (11.23[a])	6.29 (6.27[a])	108.46 (107.49[a])

Table 2 The *Γ*-point effective electron and hole masses of topmost valence band and lowest conduction band in (010) and (001) directions. The values are in units of free-electron mass m_0, and obtained from band dispersions.

Compound	m_e^{010}	m_e^{001}	m_h^{010}	m_h^{001}
Cu_2SnS_3	0.15	0.13	1.85	0.11
Cu_2GeS_3	0.24	0.18	1.01	0.18
Cu_2SiS_3	0.33	0.22	1.12	0.41

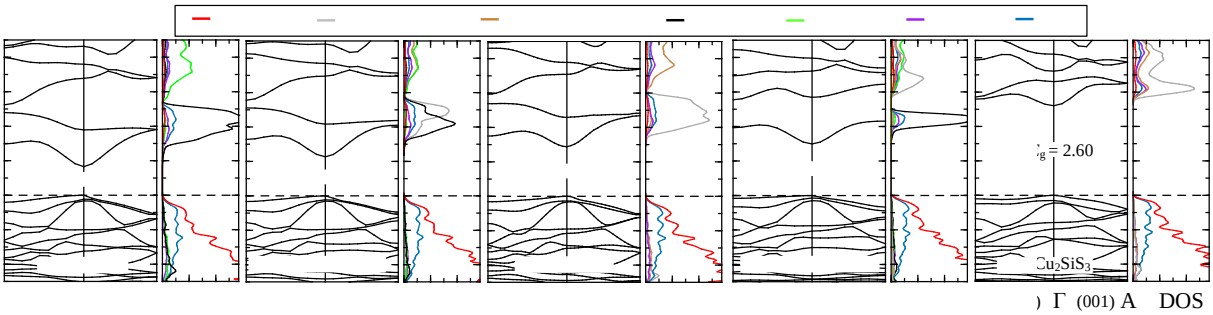

Figure 1 The electronic band structure and atom- and angular-momentum-dependent density-of-states (PDOS) for (a) Cu_2SnS_3, (b) $Cu_2Sn_{0.5}Ge_{0.5}S_3$, (c) Cu_2GeS_3, (d) $Cu_2Sn_{0.5}Si_{0.5}S_3$, (e) Cu_2SiS_3. For better visibility, the PDOS is scaled with $1/(2\ell+1)$ where ℓ is the quantum number of the angular momentum. The PDOS are presented with a 50 meV Lorentzian broadening.

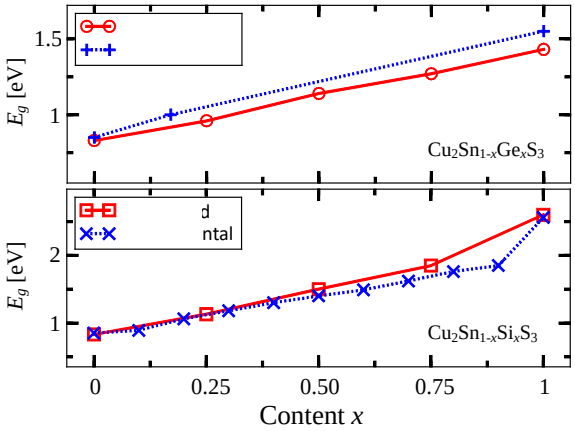

Figure 2 Calculated gap energies of $Cu_2Sn_{1-x}Ge_xS_3$ and $Cu_2Sn_{1-x}Si_xS_3$ with x = 0, 0.25, 0.5, 0.75, and 1. As comparison, available experimental values are presented [6, 8, 9].

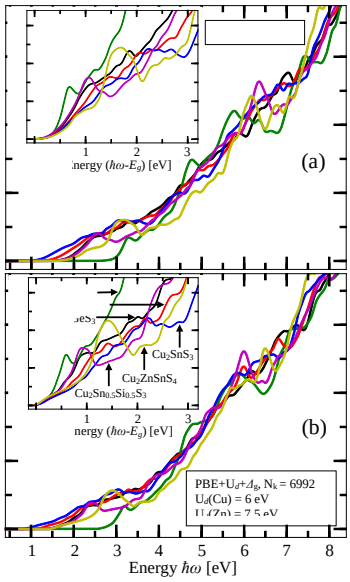

Figure 3 Calculated absorption coefficients of $Cu_2Sn_{1-x}Ge_xS_3$ and $Cu_2Sn_{1-x}Si_xS_3$ with x = 0, 0.5, and 1, using (a) HSE06 with a sparse **k**-mesh and (b) PBE+U_d with a dense **k**-mesh. For comparison, absorption of kesterite Cu_2ZnSnS_4 is presented.